International Journal of Finance & Economics

WILEY

RESEARCH ARTICLE OPEN ACCESS

Alternative Price Dynamics and Valuation of Flexible Strategies

Cristina Bertolosi[1] | Gianluca Fusai[1,2] | Ioannis Kyriakou[3]

[1]Dipartimento di Studi per l'Economia e l'Impresa, Università del Piemonte Orientale, Novara, Italy | [2]Faculty of Finance, Bayes Business School, City St George's, University of London, London, UK | [3]Faculty of Actuarial Science and Insurance, Bayes Business School, City St George's, University of London, London, UK

Correspondence: Ioannis Kyriakou (ioannis.kyriakou@city.ac.uk)

Received: 22 May 2025 | **Revised:** 17 September 2025 | **Accepted:** 17 October 2025

Keywords: investment | optimal switching | real options | uncertainty

ABSTRACT

In this article, we study the optimal operational strategy of production projects. We investigate different underlying price models and determine the optimal barriers of transition to suspension, recovery, or irreversible abandonment of productive activity. We compute probabilities of switching between alternative states and the time spent in each state. Our findings suggest that in moderately volatile markets, different model assumptions lead to minimal variations in project strategy. This insight underscores that tractable model approximations can be strategically sound under certain volatility conditions. Our work significantly advances in this direction by demonstrating when and how model simplifications can be made without sacrificing accuracy.

1 | Introduction

Selecting an appropriate model to represent economic uncertainty remains an open problem in the real options literature. This article analyzes the impact of output price dynamics modeling on optimal managerial strategies and production project valuation. We study four models, namely the inhomogeneous geometric Brownian motion (Bhattacharya 1978; Zhao 2009), the square-root mean-reverting process (Cox et al. 1985), the constant elasticity of variance process (Cox 1975), and the geometric Brownian motion.

This work advances the literature in several ways. We examine production projects with multiple options, including indefinite suspension and abandonment, highlighting the role of managerial strategy in option selection. We also introduce a rigorous comparative framework for calibrating alternative models to a benchmark, which enables meaningful evaluation. Our study demonstrates that price process specifications significantly influence transition barriers, timing, option exercise probabilities, and overall project valuation. It highlights the performance of different models in both valuation and strategy, while showing that simpler models may remain effective under offsetting mean-reversion and volatility conditions, thus preserving tractability with minimal strategic impact. Our contribution is particularly relevant to international finance. Prokopczuk et al. (2019) document significant co-movements between economic variables and commodity prices. More broadly, cross-border investments are often influenced by energy, commodities, and raw materials price dynamics. These markets are characterised by pronounced volatility, mean-reversion, seasonality, and price spikes (Roncoroni et al. 2015; Rotondi 2025a; Rotondi 2025b), which further complicate global planning and investment decisions. This volatility, exacerbated by recent geopolitical, climate-related, and health disruptions, has increasingly compelled multinational firms to reconfigure their global operations. For example, 86.2% of US manufacturers nearshored to Mexico and Canada (Deloitte 2024), over 90% shifted to emerging hubs such as India and Southeast Asia (Boston Consulting Group 2023), and EU firms strengthened supply chain resilience amid raw material shortages (European Investment

TABLE 1 | The table summarises the contributions most closely related to ours, indicating the types of real options and price models included, and positioning our article within this landscape.

Literature	Options	Models
Metcalf and Hassett (1995)	Irreversible entry	IGBM; GBM
Sarkar (2003)	Irreversible entry	IGBM; GBM
Tsekrekos (2010)	Partially reversible entry and exit	IGBM; GBM
Tsekrekos (2013)	Irreversible exit	IGBM; GBM
Tvedt (2022)	Partially reversible entry and exit	IGBM; GBM
Dias et al. (2015)	Partially reversible entry and exit	IGBM; CIR; OU
		GBM; CEV; CKLS
This article	Partially reversible entry and exit;	IGBM; CIR;
	Irreversible exit	GBM; CEV

Note: The following abbreviations are used: CEV—constant elasticity of variance; CKLS—mean-reverting CEV (Chan et al. 1992); CIR—square-root diffusion; GBM—driftless geometric Brownian motion; IGBM—inhomogeneous geometric Brownian motion; OU—Ornstein–Uhlenbeck process (Uhlenbeck and Ornstein 1930).

TABLE 2 | The table presents the price models considered in this article.

Model	SDE	$\mathcal{A}V(x)$	Θ
IGBM	$\mathrm{d}x = \kappa(\theta - x)\mathrm{d}t + \sigma x \mathrm{d}W$	$\frac{\sigma^2}{2}x^2V''(x) + \kappa(\theta - x)V'(x)$	κ, θ, σ
CIR	$\mathrm{d}x = \kappa(\theta - x)\mathrm{d}t + \sigma\sqrt{x}\mathrm{d}W$	$\frac{\sigma^2}{2}xV''(x) + \kappa(\theta - x)V'(x)$	κ, θ, σ
CEV	$\mathrm{d}x = \mu x \mathrm{d}t + \sigma x^{\beta+1}\mathrm{d}W$	$\frac{\sigma^2}{2}x^{2\beta+2}V''(x) + \mu x V'(x)$	μ, σ
GBM	$\mathrm{d}x = \sigma x \mathrm{d}W$	$\frac{\sigma^2}{2}x^2V''(x)$	μ, σ

Note: For each model, the corresponding stochastic differential equations (SDE), expressions $\mathcal{A}V(x)v^2(x) := V''(x)/2 + \delta(x)V'(x)$, and parameter sets Θ are given.

Bank 2025). Our study may also gain additional relevance and depth when situated alongside modelling approaches from the international business literature (Tong and Reuer 2007; Chi et al. 2019; Ipsmiller et al. 2021), and when interpreted in light of recent findings on supply chain disruptions and systemic risk (Le Guenedal and Tankov 2025; Amici et al. 2025).

This work aligns with research on the impact of uncertainty dynamics on investment decisions, rooted in the seminal contributions of Metcalf and Hassett (1995) and Sarkar (2003). In particular, Sarkar (2003) highlights that mean-reverting dynamics in input cost processes significantly influence investment probabilities. Tsekrekos (2010) and Tvedt (2022) reach similar conclusions in the context of revenue uncertainty and partially reversible entry and exit decisions, while Tsekrekos (2013) considers the option to irreversibly exit the market. Notably, all these studies employ the inhomogeneous geometric Brownian motion, that is, geometric mean-reverting process (see Table 2), which facilitates direct comparison of their results.

Mean-reverting dynamics are widely used in real option model settings because of their ability to capture equilibrium adjustments in price or demand functions, which are common sources of uncertainty. This has been emphasised in studies such as Bhattacharya (1978), Kulatilaka (1988), Lund (1993), Bessembinder et al. (1995), Schwartz (1997), Sarkar and Zapatero (2003), Fama and French (2000), and Ewald and Wang (2010). Nonetheless, model selection should consider the specific characteristics of the industry and the project. For example, the leverage effect, observed in stock prices (Black 1976), and the inverse leverage effect, documented in energy markets (Geman and Shih 2008; Li et al. 2017), have led to the adoption of the constant elasticity of variance process, as seen in Geman (2008), Čermák (2017), and Dias and Nunes (2011) in the real options literature. Importantly, evidence from biological (Dangerfield et al. 2018) and financial (Dias et al. 2015) contexts highlights the use of advanced models, such as the logistic and constant elasticity of variance processes, in effectively capturing the complexities of state variables' dynamics. This is crucial for determining optimal intervention or investment timing, particularly in highly volatile environments.

The previous studies focus on isolated investment decisions, such as market entry or exit, whether reversible or irreversible. However, reducing project management to a binary choice between continuation and a single alternative oversimplifies reality, as corporate strategies often encompass a broader array of options (Dixit and Pindyck 1994; Guthrie 2009). Furthermore, when multiple alternative options are available, not only the selection of an appropriate model for the underlying state variable's dynamics, but also its accurate parameterization plays a critical role in shaping business strategies. This is exemplified by Gutiérrez (2021), who shows that variations in interest rates have a non-monotonic effect on investment timing, emphasising the need for regularly updating model inputs.

This article advances the literature by presenting a more comprehensive framework that considers both multiple alternative options and different price models, unlike prior analyses that focus on only one of these aspects. Table 1 compares relevant works, outlining the real options and price models they examine and situating our study within this context. We explore a setting in which options to partially reversibly suspend (or, alternatively, resume) and to irreversibly abandon production are available. We note that reversible and irreversible decisions are mutually exclusive, and we show that the selection of which option to activate may depend on the underlying price model used. We compare the effects of different price diffusion models that are particularly relevant in the finance literature. We establish the inhomogeneous geometric Brownian motion as a benchmark and calibrate the parameters of all other price processes on it, ensuring a balanced consideration of mean and variance characteristics across the models. Our analysis examines the strategic implications of operating policies in the context of long-term projects. Specifically, we focus on three key aspects: determining the optimal prices that trigger the exercise of options, evaluating the probability of exercising real options in the short term, and analysing the timing of decisions. Also, we consider the implications for project valuation. The results vary across scenarios, as different combinations of volatility and mean reversion lead to distinct conclusions depending on the specific case.

The remainder of the article is as follows. In Section 2, we present the framework for our analysis and outline how to determine the value of the project and its optimal operating strategy. We also discuss the case of a levered project and explain why we focus on an unlevered one instead. In Section 3, we present numerical results and analyse the problem from various perspectives. Concluding remarks are provided in Section 4, whereas the derivations of results are deferred to Appendix A.

2 | Model and Methodology

We build on the entry–exit model with a scrapping option introduced in Dixit and Pindyck (1994). In this section, we present its features and adapt it to our price models. We show how to calculate the value of the project as the solution of an ordinary differential equation and according to different possible states of production. We also outline the conditions that must be satisfied to achieve the optimal managerial strategy for the project.

2.1 | The Framework

We consider an investment project that consists of producing and selling a certain good. We assume that the project value is entirely given by the selling price x, determined by the market, net of production costs. Additionally, it is widely accepted in the literature to assume an infinite time-horizon when dealing with long-lived investment projects; we adopt this line of thought.

Let $\left(\Omega, \mathscr{F}, \mathbb{F} = \left\{\mathscr{F}_t\right\}_{t\geq 0}, \mathbb{P}\right)$ be a filtered probability space, where $\mathbb{P}$ is a given probability measure. The output price process $x := \left\{x_t\right\}_{t\geq 0}$ evolves according to the stochastic differential equation

$$\mathrm{d}x = \delta(x)\mathrm{d}t + \nu(x)\mathrm{d}W, \tag{1}$$

given initial condition $x_0 \in \mathbb{R}^+$, where $W = \left\{W_t\right\}_{t\geq 0}$ is a standard Brownian motion under $\mathbb{P}$. Operating costs are constant, strictly non-negative, and given by $c = v + f$, where v denotes the variable component, directly related to production activity, and f represents the fixed cost, incurred regardless of whether production takes place (Dixit and Pindyck 1994).

Furthermore, managers can partially mitigate market fluctuations by suspending production; when this occurs, the option to restart becomes active. Following Dixit (1989), the payment of a lump sum $s_{10} \in \mathbb{R}^+$ (resp. $s_{01} \in \mathbb{R}^+$) is required to switch production from the active (resp. suspended) to the suspended (resp. active) state. The option to permanently abandon the project can be exercised at any time, whether during active or suspended production. Upon abandonment, all assets related to the project are liquidated and investors receive a fraction ηI of some initial investment cost I, where $I \in \mathbb{R}^+$ and $\eta \in [0, 1]$.

In practice, each option is exercised instantaneously when the output price reaches a critical threshold: from above, in the case of suspension and abandonment, or from below, in the case of reactivation. We denote by x_s, x_r, and x_a the price boundaries that trigger project suspension, reactivation, and abandonment, respectively. We also account for a second rigid project, with absent options to suspend and reactivate production and with abandonment occurring when the output price drops below $\overline{x}_a$. We note that if $x_s < x_a$, the managers of the flexible project behave as if it were rigid, and abandonment becomes the only relevant option. In the opposite case, the suspension option is exercised first, and the critical threshold for abandonment is lowered relative to that of the rigid project. Consequently, $\overline{x}_a$ serves as an upper bound for x_a.

2.2 | Underlying Price Dynamics and Project Value

In this work, we mainly address the implications of adopting different specifications for the process of the underlying variable x, and, in particular, we consider four models satisfying (1). Namely, our choice includes the inhomogeneous geometric Brownian motion (IGBM), the (driftless) geometric Brownian motion (GBM), the square-root (CIR) and constant elasticity of variance (CEV) diffusions.

By assumption, the value of the project, denoted by $V(x)$, depends on the cash flows it generates and on the dynamics of the underlying variable. From (1) and using Itô's lemma, we obtain the expected capital gain of the project:

$$\frac{\mathbb{E}[\mathrm{d}V]}{\mathrm{d}t} \approx \frac{\nu^2(x)}{2}V''(x) + \delta(x)V'(x) =: \mathcal{A}V(x).$$

The risk-free total return of the project, $rV(x)\,/\,\mathrm{d}t$, must equal the expected capital gain in addition to the cash flows $F(x)$ generated per unit of time. Hence,

$$\mathcal{A}V(x) = rV(x) - F(x). \tag{2}$$

We collect all stochastic differential equations for the price models, the corresponding expressions for $\mathcal{A}V(x)$, and the relevant parameter sets Θ in Table 2.

Given the price models in Table 2, the solution to (2) is of the form

$$V(x) = p\Phi(\alpha, \gamma; h(x))x^{\xi_1} + q\Phi(1 + \alpha - \gamma, 2 - \gamma; h(x))x^{\xi_2} + \psi(x), \tag{3}$$

where the first two terms are the general solution of the homogeneous equation $\mathcal{A}V(x) - rV(x) = 0$ and $\psi(x)$ is a particular solution of (2). $\Phi(\alpha, \gamma; h(x))$ is the confluent hypergeometric function of the first kind (Lebedev 1972). The parameters $\xi_1, \xi_2 \in \mathbb{R}$ depend on the dynamics of x, while $p, q \in \mathbb{R}$ are constant coefficients to be determined via appropriate boundary conditions.

2.3 | The State-Dependent Valuation Problem

It is important to note that cash flows depend on the operational state of the project. In particular, we have that $F(x) = x - c$ when production takes place, and $F(x) = -f$ while it is suspended. Consequently, the value of the project differs accordingly. Let $V_1(x)$ and $V_0(x)$ be the value of the project when production is active and suspended, respectively. Then, $V_1(x)$ solves

$$\mathcal{A}V_1(x) = rV_1(x) - (x - c) \tag{4}$$

subject to $\lim_{x\to+\infty} V_1(x) < \infty$, whereas $V_0(x)$ is the solution of

$$\mathcal{A}V_0(x) = rV_0(x) + f \tag{5}$$

subject to $\lim_{x\to 0^+} V_0(x) < \infty$. The two conditions prevent the value of the project from exploding as the output price either increases or approaches zero, respectively. From an economic perspective, this implies that the value of the option to suspend (respectively, restart) production, available while the project is in the active (respectively, suspended) state, decreases as the output price rises (respectively, converges to zero). When this is the case, the project value converges to $\psi(x) = \mathbb{E}\left[\int_0^\infty F(x)e^{-ru}\,\mathrm{d}u\right]$. Finally, the project value at the time of abandonment equals the scrap value ηI, regardless of the underlying price dynamics.

Next, we present the value functions for the active project, $V_1(x)$, and the suspended project, $V_0(x)$, across all relevant price models. Recall that when production is suspended, the instantaneous cash flow is $-f$, leading to $\psi(x) = -f\,/\,r$, independently of the specific model. Conversely, when production is active,

$$\psi(x) = \begin{cases} \dfrac{x}{r+\kappa} + \dfrac{\theta}{r} - \dfrac{\theta}{(r+\kappa)} - \dfrac{c}{r} & \text{if } MR \\ \dfrac{x}{r-\mu} - \dfrac{c}{r} & \text{if } \overline{MR} \end{cases},$$

where MR and $\overline{MR}$ are used to distinguish between the mean-reverting and non-mean-reverting cases. In what follows, we accordingly adopt $\psi^{MR}(x)$ and $\psi^{\overline{MR}}(x)$. To simplify notation, we use $\alpha_{1,2}$, $\gamma_{1,2}$, and $\xi_{1,2}$ uniformly across all models. However, the specific values of these parameters vary depending on the stochastic process assumed for the underlying variable; their derivation is provided in Appendix A. Similarly, we use $q_{1,2}$ and $p_{1,2}$ to denote parameters whose values also vary by model.

For the benchmark IGBM model, we obtain the solutions

$$V_1(x) = q_2\Phi\left(\alpha_2, \gamma_2; \frac{2\kappa\theta}{\sigma^2 x}\right)x^{\xi_2} + \psi^{MR}(x),$$
$$V_0(x) = p_1x^{\xi_1}\Phi\left(\alpha_1, \gamma_1; \frac{2\kappa\theta}{\sigma^2 x}\right) + p_2x^{\xi_2}\Phi\left(\alpha_2, \gamma_2; \frac{2\kappa\theta}{\sigma^2 x}\right) - \frac{f}{r}.$$

Under the CIR model, we obtain

$$V_1(x) = \widetilde{q}_2\Phi\left(\alpha_2, \gamma_2; \frac{2\kappa x}{\sigma^2}\right)x^{\xi_2} - \widetilde{q}_1\Phi\left(\alpha_1, \gamma_1; \frac{2\kappa x}{\sigma^2}\right)x^{\xi_1} + \psi^{MR}(x),$$
$$V_0(x) = p_1\Phi\left(\alpha_1, \gamma_1; \frac{2\kappa x}{\sigma^2}\right) + p_2\Phi\left(\alpha_2, \gamma_2; \frac{2\kappa x}{\sigma^2}\right)x^{\xi_2} - \frac{f}{r},$$

where

$$\widetilde{q}_1 = q_2\left(\frac{2k}{\sigma^2}\right)^{1-\gamma_2}\frac{\Gamma(\gamma_2)\Gamma(1-\gamma_2)}{\Gamma(\alpha_2)\Gamma(\gamma_1)},$$
$$\widetilde{q}_2 = q_2\frac{\Gamma(1-\gamma_2)}{\Gamma(\gamma_1)}.$$

If the underlying price process follows a GBM, then the solutions are

$$V_1(x) = q_2x^{\xi_2} + \psi^{\overline{MR}}(x)$$
$$V_0(x) = p_1x^{\xi_1} + p_2x^{\xi_2} - \frac{f}{r}.$$

Finally, in the case of CEV, the signs of parameters μ and β must be considered, leading to the following expressions:

$$V_1(x) = \begin{cases} \left[\widetilde{q}_1\Phi\left(\alpha_1;\gamma_1, \dfrac{\mu}{|\beta|\sigma^2x^{2\beta}}\right)x^{\xi_1} + \widetilde{q}_2\Phi\left(\alpha_2;\gamma_2, \dfrac{\mu}{|\beta|\sigma^2x^{2\beta}}\right)x^{\xi_2}\right]e^{\frac{\mu}{\beta\sigma^2x^{2\beta}}\mathbf{1}_{\{\beta<0\}}} + \psi^{\overline{MR}}(x) & \text{if } \mu \neq 0 \\ \left[\widetilde{q}_1\Phi\left(\alpha_1;\gamma_1, \dfrac{2\sqrt{2r}}{|\beta|\delta x^{\beta}}\right)x^{\xi_1} + \widetilde{q}_2\Phi\left(\alpha_2;\gamma_2, \dfrac{2\sqrt{2r}}{|\beta|\delta x^{\beta}}\right)x^{\xi_2}\right]e^{\frac{\sqrt{2r}}{|\beta|\delta x^{\beta}}} + \psi^{\overline{MR}}(x) & \text{if } \mu = 0 \end{cases},$$

and

$$V_0(x)=\begin{cases}\left[\widetilde{p}_1\Phi\left(\alpha_1;\gamma_1,\frac{\mu}{|\beta|\sigma^2x^{2\beta}}\right)x^{\xi_1}+\widetilde{p}_2\Phi\left(\alpha_2;\gamma_2,\frac{\mu}{|\beta|\sigma^2x^{2\beta}}\right)x^{\xi_2}\right]e^{\frac{\mu}{\beta\sigma^2x^{2\beta}}\mathbf{1}_{\{\beta<0\}}}+\psi(x) & \text{if } \mu\neq 0\\ \left[\widetilde{p}_1\Phi\left(\alpha_1;\gamma_1,\frac{2\sqrt{2r}}{|\beta|\sigma x^{\beta}}\right)x^{\xi_1}+\widetilde{p}_2\Phi(\alpha_2;\gamma_2,2z)x^{\xi_2}\right]e^{-\frac{2\sqrt{2r}}{|\beta|\sigma x^{\beta}}} & \text{if } \mu=0\end{cases},$$

where

$$\begin{aligned}
&\widetilde{q}_1=q_2\frac{\Gamma(1-\gamma_1)}{\Gamma(\alpha_2)},\quad \widetilde{q}_2=\left(-\frac{\mu}{\beta\sigma^2}\right)^{1-\gamma_1}\frac{\Gamma(\gamma_1-1)}{\Gamma(\alpha_1)} && \text{if } \mu\neq 0,\beta<0,\\
&\widetilde{q}_1=0,\quad \widetilde{q}_2=q_3\in\mathbb{R} && \text{if } \mu\neq 0,\beta>0,\\
&\widetilde{q}_1=q_2\frac{\sqrt{\pi}\Gamma\left(\frac{1}{\beta}\right)}{\Gamma\left(\frac{\beta+1}{2\beta}\right)}\left(-\frac{2\sqrt{2r}}{\sigma\beta}\right)^{-\frac{1}{2\beta}},\quad \widetilde{q}_2=0 && \text{if } \mu=0,\beta<0,\\
&\widetilde{q}_1=q_2\frac{\sqrt{2r}}{2^{\frac{1}{2\beta}}\sigma\beta\Gamma\left(\frac{1}{2\beta}+1\right)},\quad \widetilde{q}_2=q_2\frac{\Gamma\left(-\frac{1}{\beta}\right)}{\Gamma\left(\frac{\beta-1}{2\beta}\right)}2^{-\frac{1}{2\beta}}\sqrt{\pi}\left(-\frac{\sqrt{2r}}{\sigma\beta}\right)^{\frac{1}{2\beta}} && \text{if } \mu=0,\beta>0,
\end{aligned}$$

and

$$\widetilde{p}_1=\left[p_1\sqrt{\pi}2^{\frac{1}{2|\beta|}}\frac{\Gamma\left(-\frac{1}{|\beta|}\right)}{\Gamma\left(\frac{1}{2}-\frac{1}{2|\beta|}\right)}+p_2\frac{1}{2^{\frac{1}{2|\beta|}}\Gamma\left(\frac{1}{2|\beta|}+1\right)}\right]\frac{2\sqrt{2r}}{|\beta|\sigma},$$

$$\widetilde{p}_2=p_1 2^{\frac{1}{2|\beta|}}\frac{\Gamma\left(\frac{1}{2|\beta|}\right)}{\Gamma\left(\frac{1}{2}+\frac{1}{2|\beta|}\right)}\frac{2\sqrt{2r}}{|\beta|\sigma x^{\beta}}.$$

Fuller details of the presented solutions can be found in Appendix A.

2.4 | Optimal Switching Boundaries

At any given moment, managers decide whether to exercise an option by comparing the project's continuation value with the value achievable through switching, in order to maximise profits. The continuation value equals $V_1(x)$ when the project is active and $V_0(x)$ when suspended, net of the appropriate switching cost s_{10} or s_{01}. Additionally, since project abandonment is irreversible, it can only be considered as an alternative to keeping the project active or suspended. Moreover, the value of the project is driven by the uncertain behaviour of the output price: it turns out that we need to determine three critical values of x, namely, x_s, x_r, x_a ($\overline{x}_a$ for the rigid project), that trigger switching decisions. Noticeably, in correspondence of such boundaries, managers are indifferent between continuation and switching; hence, the continuation value must be equal to the alternative one, net of switching costs. Consequently, we get the following boundary conditions for $V_1(x)$ and $V_0(x)$:

$$\begin{cases}V_1(x_s)=V_0(x_s)-s_{10}\\ V_0(x_r)=V_1(x_r)-s_{01}\\ V_0(x_a)=\eta I\end{cases}. \tag{6}$$

Additionally, for x_s, x_r, x_a to be optimal, the smooth-pasting conditions must also be satisfied[1]:

$$\begin{cases}V_1'(x_s)=V_0'(x_s)\\ V_0'(x_r)=V_1'(x_r)\\ V_0'(x_a)=0\end{cases}. \tag{7}$$

Clearly, when the project is rigid, or whenever it is optimal to immediately exercise abandonment without previously suspending, systems (6) and (7) reduce to

$$V_1(\overline{x}_a)=\eta I \tag{8}$$

and

$$V_1'(\overline{x}_a)=0. \tag{9}$$

Solving Equations (6) and (7) (respectively, Equations (8) and (9)) for the constant coefficients, as well as for x_s, x_r, x_a (respectively, $\overline{x}_a$), yields the optimal managerial strategy for a given model.

2.5 | The Levered Case

The model presented in Section 2 refers to a project entirely financed by equity. Here, we consider the case of presence of debt. To this end, we assume that the project is partially funded by means of a perpetual bond with continuous coupon C; possibly, a tax-shield exists for a constant tax-rate ϑ. Abandoning the project implies default on debt, with the payment of some recovery value to bondholders and no residual value to equity holders. The price that optimally triggers default is x_d. The value of the project's assets is the sum of equity and debt, that is, $V(x)=E(x)+D(x)$, where $E(x)$ is the equity value, $D(x)$ the debt value, and both depend on the instantaneous output price and increase with the risk-free rate r. Hence, they satisfy the ordinary differential equations

$$\mathcal{A}E(x)=rE(x)-F(x)+C(1-\vartheta) \tag{10}$$

and

$$\mathcal{A}D(x)=rD(x)-C, \tag{11}$$

where $F(x)$ denotes the same cash flow as in Equation (2) and $\mathcal{A}E(x)=\mathcal{A}D(x)=\mathcal{A}V(x)$ as in Table 2. Compared to the all-equity case, the only difference for equity holders is a reduction in earnings equal to $C(1-\vartheta)$. Conversely, bondholders receive a constant coupon payment C until default. In the event of default, the project's assets are liquidated, and bondholders are partially reimbursed through the proceeds of the sale. We denote this by $\omega V(x_d)$, where $V(x_d)$ is the value of an all-equity project for $x=x_d$ and $\omega\in[0,1]$. Equation (11) is solved subject to the boundary conditions

$$
\begin{cases}
\lim_{x\to\infty} D(x) = \mathbb{E}\left[\int_0^{+\infty} Ce^{-ru}\,\mathrm{d}u\right] = \frac{C}{r}\,. \\
D(x_d) = \omega V(x_d)
\end{cases}
$$

Note that none of the preceding conditions is imposed at the suspension or resumption boundaries. Additionally, the default boundary is exogenous to bondholders. Indeed, decision-makers are assumed to be equity holders or managers acting on their behalf. Consequently, operational decisions are made to maximise the value of equity, rather than the value of the project's assets. This implies that Equation (10) must be solved subject to the value-matching conditions

$$
\begin{cases}
E_1(x_s) = E_0(x_s) - s_{10} \\
E_0(x_r) = E_1(x_r) - s_{01}\,, \\
E_0(x_d) = 0
\end{cases}
\tag{12}
$$

and smooth-pasting conditions

$$
\begin{cases}
E_1'(x_s) = E_0'(x_s) \\
E_0'(x_r) = E_1'(x_r)\,. \\
E_0'(x_d) = 0
\end{cases}
\tag{13}
$$

In practice, any impact of debt on the suspension and restart boundaries can be excluded. This depends on the coupon being paid independently from production being active or suspended, which can be verified analytically by solving (12) and (13). All else being equal, the default price of a levered firm is higher than the liquidation price of an unlevered firm since the coupon payment reduces equity cash flows. In sum, the only effect of introducing debt into the analysis is a reduction in equity holders' cash flows, regardless of whether production is ongoing or suspended. However, this effect can be equivalently achieved by increasing the level of fixed costs f in the baseline all-equity framework.

On the other hand, our assumption of managers maximizing equity value gives rise to a second-best optimal strategy for the project. Recently, Glover and Hambusch (2016) and Ritchken and Wu (2021) obtained first-best solutions for similar problems by maximizing the total asset value under output prices evolving, respectively, as an IGBM and a GBM with drift. Moreover, they determined the optimal coupon on debt, which we assume as given. Additionally, in the presence of an option to relocate investments across borders, it would also be of interest to relax the assumption of a constant tax rate, allowing it instead to be uncertain. In this regard, Azevedo et al. (2019) underscore the importance of stable and predictable tax policies in attracting foreign investment, and suggest that well-designed tax holidays can significantly influence investment decisions. This result is expected to influence the optimal level of financial leverage or, equivalently, the amount of debt a firm can raise.

Indeed, determining the project's optimal financing strategy lies beyond the scope of this work; nevertheless, we identify it as a direction for future research, particularly given the valuable insights into firms' creditworthiness that can be gained through the analysis of financial leverage.

3 | Results and Discussion

In this section, we numerically investigate how different price models influence the project's optimal strategy, focusing on the real options' exercise boundaries, the probabilities of implementing the optimal strategy within a short horizon, and the timing of decisions. We also examine the implications for project value and assess the sensitivity of our results to changes in the project's degree of flexibility. Table 3 presents the set of parameters that, unless otherwise specified, are held unchanged throughout the analysis. The parameter values we adopt are consistent with those commonly used in the literature (see, e.g., Tsekrekos 2010, 2013).

3.1 | Model Calibration

A standard approach in the literature involves comparing different models by maintaining identical values for parameters common among processes. For instance, Sarkar (2003) and Tsekrekos (2010) compare the outcomes of an IGBM with those of a driftless GBM, assuming the same volatility parameter σ. While this may be reasonable to some extent, it is less straightforward to justify the choice made by Dias et al. (2015) and Dangerfield et al. (2018), who keep same key parameters across processes with fundamentally different specifications.

Instead, an effective comparative analysis should be conducted among models that exhibit similar features. For instance, introducing mean-reversion typically reduces the variance of a process for a given volatility parameter. A preliminary examination of price dynamics should aim to fit a model that matches empirical observations as closely as possible; alternatively, a particular process may be assumed a priori. Moreover, even an analyst who correctly identifies the dynamics may replace it with a process that is simpler to handle. Nevertheless, the new process must be calibrated so that it retains the main features of the empirical one.

TABLE 3 | The table compiles and describes the parameters used for the numerical implementation of the model.

Notation	Value	Description
r	0.04	Risk-free rate
v	1.7	Production cost of the project
f	0.1	Fixed cost of the project
I	20	Initial cost of the project
η	0.5	Recovery fraction of cost I upon project liquidation
s_{10}	0.1	Cost to switch from production to suspension
s_{01}	0.2	Cost to switch from suspension to production

To this end, we propose calibrating our models as follows. First, we choose the IGBM model as the benchmark, as it is widely used in the literature and offers a realistic representation of price time series. Next, we compute the first and second raw moments of the logarithm of this process, as well as those of the k-th model for $k \in \{\text{CIR}, \text{CEV}(\beta), \text{GBM}\}$. Finally, we determine the values of the set of parameters Θ, specified in Table 2 for each k-th model, by solving

$$\min_{\Theta} \left\{ \sum_{j=1}^{T} \left[\mu_j^1(k,\Theta) - \mu_j^1\left(\Theta^{\text{IGBM}}\right)\right]^2 + \frac{1}{4} \sum_{j=1}^{T} [\mu_j^2(k,\Theta) - \mu_j^2\left(\Theta^{\text{IGBM}}\right)]^2 \right\}$$

for $\mu_j^n = \mathbb{E}\left[\ln\left(x_j\right)^n \mid \mathscr{F}_0\right]$, for the indicated model, considering a total of T horizons. Working with log-prices is common, as log-changes are often much closer to being stationary than raw price changes, ensuring greater stability; this also naturally aligns with exponential price models, and the required moments are more readily available in log-space (see, for example, discussion on the moment problem in Kyriakou et al. 2023). Eight horizons (1, 2, 3, 5, 10, 15, 20, and 30 years) are selected, in line with standard practice, to capture short-, medium-, and long-term project lifespans. The weighting coefficient $1/4$ has been empirically chosen to balance the two terms in the objective function, ensuring stable convergence of the numerical optimization.

We analyse three scenarios characterised by different interactions between the mean-reversion speed κ and the volatility parameter σ. In the first scenario, with $(\kappa, \sigma) = (0.30, 0.15)$, the relatively higher mean-reversion speed compared to volatility implies stronger pull-back dynamics in the price process. By comparison, the pair $(\kappa, \sigma) = (0.07, 0.30)$ corresponds to a setting where volatility dominates relative to mean-reversion. Finally, an intermediate scenario is given by $(\kappa, \sigma) = (0.15, 0.20)$. We apply our calibration procedure, with results reported in Table 4. As quite expected, minimal adjustments are required when transitioning from the IGBM to the CIR process. However, a significant reduction in the instantaneous volatility coefficient is necessary to offset the explosive nature of non-mean-reverting processes, particularly when the reversion rate is high in the benchmark case.

3.2 | Effect on Optimal Boundaries

Table 5 reports the optimal boundaries for the flexible project and, as a benchmark, for its rigid counterpart. Importantly, the last column indicates whether reversible suspension is actually included in the firm's optimal strategy. Evidently, selecting a model different from the IGBM benchmark results in a shift between suspension and abandonment only in a few cases. However, the abandonment threshold is considerably more sensitive to changes in the variance of the price process compared to the suspension boundary. As also noted by Tsekrekos (2013), this difference stems from the irreversible nature of abandonment, which tends to be postponed when price volatility is sufficiently high to allow for potential recovery from losses. By contrast, the option to reverse the decision makes both suspension and resumption less responsive to such variations. Consequently, we observe a marked reduction in the abandonment threshold when

TABLE 4 | The table presents the parameter values for all models under analysis.

Model	Scenario 1				Scenario 2				Scenario 3			
	κ	θ	σ	μ	κ	θ	σ	μ	κ	θ	σ	μ
IGBM	0.3	1.8	0.15		0.15	1.8	0.2	—	0.07	1.8	0.3	—
CIR	0.30699	1.79986	0.20202	—	0.16281	1.79434	0.26551	—	0.10235	1.69053	0.37328	—
GBM	—	—	0.09273	—	—	—	0.11031	—	—	—	0.16758	—
CEV($\beta = -2$)	—	—	0.19037	0.00000	—	—	0.21128	0.00000	—	—	0.26476	0.00000
CEV($\beta = -0.5$)	—	—	0.11075	0.00000	—	—	0.12716	0.00000	—	—	0.19098	0.00000
CEV($\beta = 0$)	—	—	0.04227	−0.00524	—	—	0.11032	0.00000	—	—	0.14749	−0.00565
CEV($\beta = 0.5$)	—	—	0.03177	−0.00520	—	—	0.05738	−0.00475	—	—	0.12797	0.00001
CEV($\beta = 1.5$)	—	—	0.03389	0.00002	—	—	0.03722	0.00001	—	—	0.05487	0.00002

Note: The IGBM process serves as the benchmark, with the remaining models calibrated accordingly.

TABLE 5 | The table reports the optimal abandonment x_a, suspension x_s, and resumption x_r thresholds of the flexible project, alongside the abandonment threshold $\overline{x}_a$ of an otherwise equivalent rigid project.

Panel A: IGBM parameter values $\kappa = 0.30, \sigma = 0.15$					
Model	$\overline{x}_a$	x_a	x_s	x_r	**Suspend**
IGBM	1.92476	1.92476	1.44852	1.96248	No
CIR	1.95865	1.95865	1.43154	1.95553	No
GBM	1.58730	1.58730	1.53379	1.89496	No
CEV($\beta = -0.5$)	1.65871	1.65871	1.19290	2.01668	No
CEV($\beta = 0$)	1.99913	1.99913	1.60244	1.91355	No
CEV($\beta = 0.5$)	1.87485	1.87485	1.60169	1.81494	No
Panel B: IGBM parameter values $\kappa = 0.15, \sigma = 0.20$					
Model	$\overline{x}_a$	x_a	x_s	x_r	**Suspend**
IGBM	1.61305	1.61305	1.42419	2.03507	No
CIR	1.67350	1.67350	1.40484	2.01944	No
GBM	1.49308	1.48127	1.51492	1.92030	Yes
CEV($\beta = -0.5$)	1.58528	1.58517	1.21306	1.97321	No
CEV($\beta = 0$)	1.49302	1.48128	1.51511	1.92017	Yes
CEV($\beta = 0.5$)	1.66345	1.66345	1.55848	1.87358	No
Panel C: IGBM parameter values $\kappa = 0.07, \sigma = 0.30$					
Model	$\overline{x}_a$	x_a	x_s	x_r	**Suspend**
IGBM	1.11047	0.93379	1.36080	2.15801	Yes
CIR	1.28974	1.23948	1.34818	2.11314	Yes
GBM	1.22664	1.11321	1.46148	1.99704	Yes
CEV($\beta = -0.5$)	1.31758	1.25818	1.33363	1.72098	Yes
CEV($\beta = 0$)	1.42044	1.38913	1.48418	1.97782	Yes
CEV($\beta = 0.5$)	1.24320	1.14523	1.47271	2.01351	Yes

Note: The last column indicates whether suspension is included in the optimal strategy. Panels A, B, and C correspond to low-, medium-, and high-volatility scenarios, respectively, defined by different combinations of the IGBM parameters κ and σ. All other model parameters are as specified in Table 3.

moving from the low-variance scenario in Panel A to the high-variance case in Panel C. Most notably, the distance between the suspension and abandonment thresholds exhibits a U-shaped pattern, highlighting the critical nature of intermediate cases. Specifically, when neither the drift nor the diffusion component dominates in the benchmark model, this gap becomes narrow, making shifts between the two boundaries more likely and sensitive to parameter changes. This is illustrated in the GBM case in Panel B, where suspension becomes part of the optimal strategy of the project despite only an average change of about 7% in the relevant thresholds compared to the IGBM benchmark.

3.3 | Effect on Entry and Exit Probabilities

We further compute the probabilities of suspending, restarting, and abandoning production within the short term, which we define as the next 5 years within the 30-year horizon. The standard approach (see Tsekrekos 2010; Dias et al. 2015) involves simulating trajectories for each model under consideration, superimposing the corresponding boundaries, and estimating probabilities by counting the frequency of state transitions. Our method is conceptually similar; however, we simulate cash flows only under the benchmark process and apply all boundaries to it. While the standard methodology may be more appropriate during a planning stage, the approach proposed here provides a more realistic representation of the project's operational behavior.

The results are presented in Table 6. Variations across models are particularly sizeable in the two extreme scenarios of low and high price volatility. The GBM, in particular, provides the weakest fit relative to the benchmark, notably overestimating the probability of multiple transitions between the active and suspended states. Nevertheless, this discrepancy is smaller under the intermediate volatility scenario. It is also worth noting that the rigid project is less sensitive to model specification than the flexible one.

TABLE 6 | The table reports the probabilities of abandonment, suspension, and restart of production in the next five years.

Model	P(A| rig)	P(A| flex)	$P(\mathrm{S} \geq 1)$	$P(\mathrm{S} > 1)$	$P(\mathrm{R} \geq 1)$	$P(\mathrm{R} > 1)$
Panel A: IGBM parameter values $\kappa = 0.30$, $\sigma = 0.15$						
IGBM	97.708	97.708	0	0	0	0
CIR	98.777	98.777	0	0	0	0
GBM	64.427	64.427	0	0	0	0
CEV($\beta = -0.5$)	75.276	75.276	0	0	0	0
CEV($\beta = 0$)	99.749	99.749	0	0	0	0
CEV($\beta = 0.5$)	95.545	95.545	0	0	0	0
Panel B: IGBM parameter values $\kappa = 0.15$, $\sigma = 0.20$						
IGBM	74.334	74.334	0	0	0	0
CIR	79.864	79.864	0	0	0	0
GBM	62.001	60.640	62.166	2.150	4.738	0.157
CEV($\beta = -0.5$)	71.587	71.587	0	0	0	0
CEV($\beta = 0$)	61.993	60.641	62.227	2.165	4.770	0.161
CEV($\beta = 0.5$)	78.935	78.935	0	0	0	0
Panel C: IGBM parameter values $\kappa = 0.07$, $\sigma = 0.30$						
IGBM	48.053	32.641	67.573	5.211	17.702	0.616
CIR	62.569	58.659	66.712	2.633	7.318	0.199
GBM	57.662	48.267	74.519	14.667	27.125	4.134
CEV($\beta = -0.5$)	64.553	60.131	65.642	6.129	9.929	0.876
CEV($\beta = 0$)	71.777	69.608	75.912	7.170	11.624	1.021
CEV($\beta = 0.5$)	58.932	51.031	75.202	14.378	26.240	3.975

Note: These values are computed numerically via Monte Carlo simulation, using $x_0 = 2.00$, 100,000 trajectories, a 30-year horizon, and 250 time steps per year. The probability of abandonment is calculated conditional on the project being either rigid P(A| rig) or flexible P(A| flex), while $P(\mathrm{S} \geq 1)$ and $P(\mathrm{S} > 1)$ refer to the probability that suspension occurs at least once or more than once, respectively. Analogously, the label "R" denotes restart. All values are expressed in percentage terms.

In summary, the choice of the model has a substantial impact on short-term entry and exit probabilities. To assess how this influences the overall project strategy, the next section focuses on estimating the project's time to abandonment.

3.4 | Effect on Timing of Strategic Decisions

To fully understand the impact of different models on the project strategy, we compute its expected time to abandonment, defined as the time until the abandonment threshold is first crossed, triggering the liquidation of the project. In addition, we calculate the percentage of time the project remains in the pre-abandonment phase over a 30-year horizon. Conditional on the project remaining alive, we further examine the durations the project spends in the active and suspended states.

The results are presented in Table 7. Once again, the most significant deviations occur under the GBM and CEV models in the low-variance scenario, confirming that these are particularly unreliable proxies for the benchmark in such cases. In the intermediate- and high-variance environments, abandonment occurs within 2.5 years of difference between models for the rigid project and within 4 years for the flexible one. Although non-negligible, these deviations are relatively modest when compared to the overall 30-year horizon. Moreover, the profile of the cumulative time spent in the active and suspended states appears very similar across all cases, indicating that small differences in time to abandonment do not necessarily result in substantial changes to the project strategy, as long as the project remains alive. The GBM case in Panel B is particularly noteworthy: while this is the only instance in which suspension is included in the project's strategy, it is evident that suspension merely acts as a preliminary step towards irreversible abandonment, with the project remaining in this state for less than 4 months in total.

Notably, the qualitative conclusions regarding abandonment behaviour are robust to the choice of the initial value, x_0, of the price process. Setting this just above the highest abandonment threshold, corresponding to the scenario with the smallest

TABLE 7 | The table reports the expected time to abandonment of the project $\left(\tau_{x_a}, \tau_{\bar{x}_a}\right)$, the percentage of time spent in the pre-abandonment state relative to a 30-year horizon $\left(\% \tau_{x>x_a}, \% \tau_{x>\bar{x}_a}\right)$, and the percentage of time spent in the active or suspended state before abandonment $\left(\% \tau_{\text{act}}, \% \tau_{\text{sus}}\right)$.

Panel A: IGBM parameter values $\kappa = 0.30$, $\sigma = 0.15$

Model	$\tau_{\bar{x}_a}$ (years)	$\tau_{x>\bar{x}_a}$ (%)	τ_{x_a} (years)	$\tau_{x>x_a}$ (%)	τ_{act} (%)	τ_{sus} (%)
IGBM	0.64925	2.164	0.64925	2.164	100	0
CIR	0.37887	1.263	0.37887	1.263	100	0
GBM	5.07987	16.933	5.07987	16.933	100	0
CEV($\beta = -0.5$)	3.73901	12.463	3.73901	12.463	100	0
CEV($\beta = 0$)	0.09609	0.320	0.09609	0.320	100	0
CEV($\beta = 0.5$)	1.08167	3.606	1.08167	3.606	100	0

Panel B: IGBM parameter values $\kappa = 0.15$, $\sigma = 0.20$

Model	$\tau_{\bar{x}_a}$ (years)	$\tau_{x>\bar{x}_a}$ (%)	τ_{x_a} (years)	$\tau_{x>x_a}$ (%)	τ_{act} (%)	τ_{sus} (%)
IGBM	4.18030	13.934	4.18030	13.934	100	0
CIR	3.37894	11.263	3.37894	11.263	100	0
GBM	6.02549	20.085	6.23044	20.768	95.406	4.594
CEV($\beta = -0.5$)	4.57443	15.248	4.57601	15.253	100	0
CEV($\beta = 0$)	6.02678	20.089	6.23037	20.768	95.381	4.619
CEV($\beta = 0.5$)	3.51263	11.709	3.51263	11.709	100	0

Panel C: IGBM parameter values $\kappa = 0.07$, $\sigma = 0.30$

Model	$\tau_{\bar{x}_a}$ (years)	$\tau_{x>\bar{x}_a}$ (%)	τ_{x_a} (years)	$\tau_{x>x_a}$ (%)	τ_{act} (%)	τ_{sus} (%)
IGBM	8.80221	29.341	11.73235	39.108	64	36
CIR	6.41350	21.378	7.02868	23.429	88	12
GBM	7.19449	23.982	8.76210	29.207	69.686	30.314
CEV($\beta = -0.5$)	6.09465	20.315	6.78857	22.629	93	7
CEV($\beta = 0$)	4.94099	16.470	5.28362	17.612	88.783	11.217
CEV($\beta = 0.5$)	6.98382	23.279	8.29358	27.645	71	29

Note: Values are computed numerically via Monte Carlo simulation, using $x_0 = 2.00$, 100,000 trajectories, a 30-year horizon, and 250 time steps per year.

volatility (Panel A in Tables 6 and 7), marginally increases the probability of early abandonment but does not affect the key finding: the ordering of the x_a levels, that is, highest in Panel A, intermediate in Panel B, and lowest in Panel C, is consistently preserved.

3.5 | Sensitivity to Flexibility-Related Costs

Next, we assess the sensitivity of our results to the degree of project flexibility. A project is considered more flexible when the costs associated with switching between the active and suspended states are lower. Similarly, lower fixed costs enhance flexibility by reducing the magnitude of negative cash flows incurred during suspension.

As a preliminary illustration, Figure 1 displays the optimal boundaries of the flexible project under the IGBM model for values of $s_{10} \in [0,0.15]$. For simplicity, we assume that restarting production is as costly as suspending it, that is, $s_{01} = s_{10}$. It is well known that under costless reversibility, production is suspended (resumed) as soon as earnings become negative (positive), implying $x_s = x_r = v$. Conversely, higher switching costs lower (raise) the suspension (resumption) threshold, thereby widening the gap between the two boundaries. This mechanism of *hysteresis* is discussed in detail in Dixit (1989) and Dias et al. (2015). We observe that greater variance in the price process amplifies the hysteresis effect. As expected, the decline in the suspension threshold is accompanied by a moderate increase in the abandonment barrier.

In contrast, the decision of when to suspend or restart production is largely insensitive to changes in the project's fixed costs. In fact, the amount f is paid regardless of whether production is active. As shown in Figure 2, an increase in f, which effectively reduces earnings, leads to a higher abandonment threshold for both the flexible and the rigid project.

The reasons for these behaviours are purely economic and can therefore be considered qualitatively valid across all the price

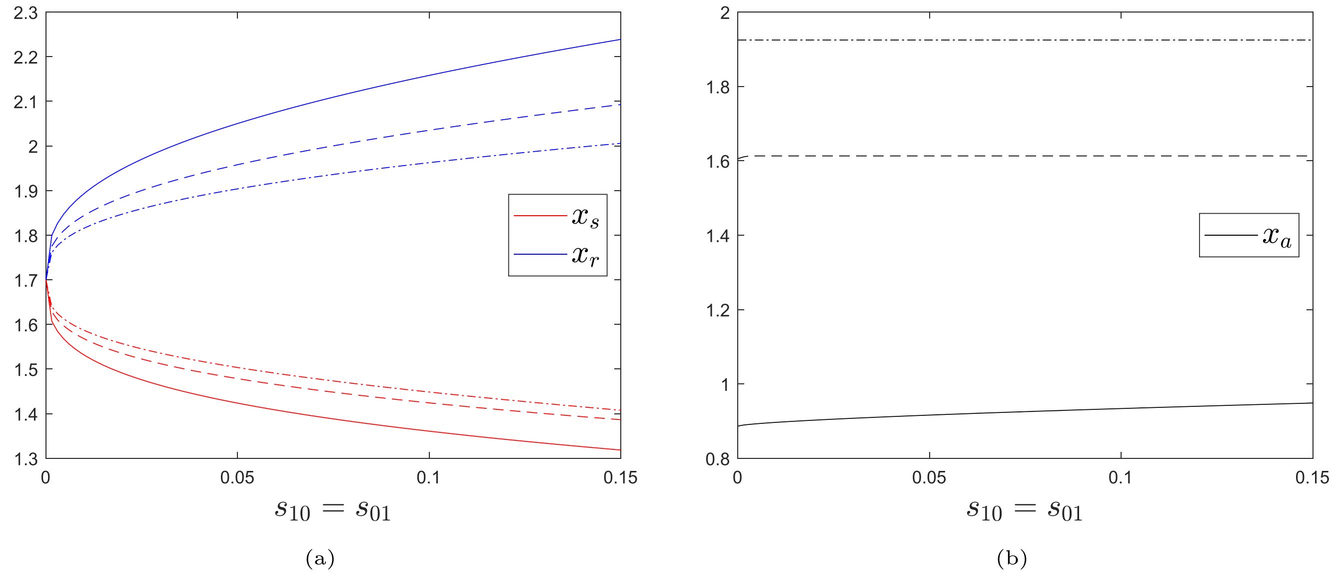

FIGURE 1 | Panel (a) displays the suspension and resumption boundaries, x_s and x_r, as functions of the suspension cost s_{10}. In Panel (b), the same is shown for the abandonment boundary x_a. Low (dash-dotted lines), intermediate (dashed lines), and high (solid lines) volatility scenarios correspond to the parameter pairs $(\kappa, \sigma) = (0.30, 0.15)$, $(\kappa, \sigma) = (0.15, 0.20)$, and $(\kappa, \sigma) = (0.07, 0.30)$, respectively. The cost to restart production is assumed equal to the cost of suspension, that is, $s_{01} = s_{10}$. [Colour figure can be viewed at wileyonlinelibrary.com]

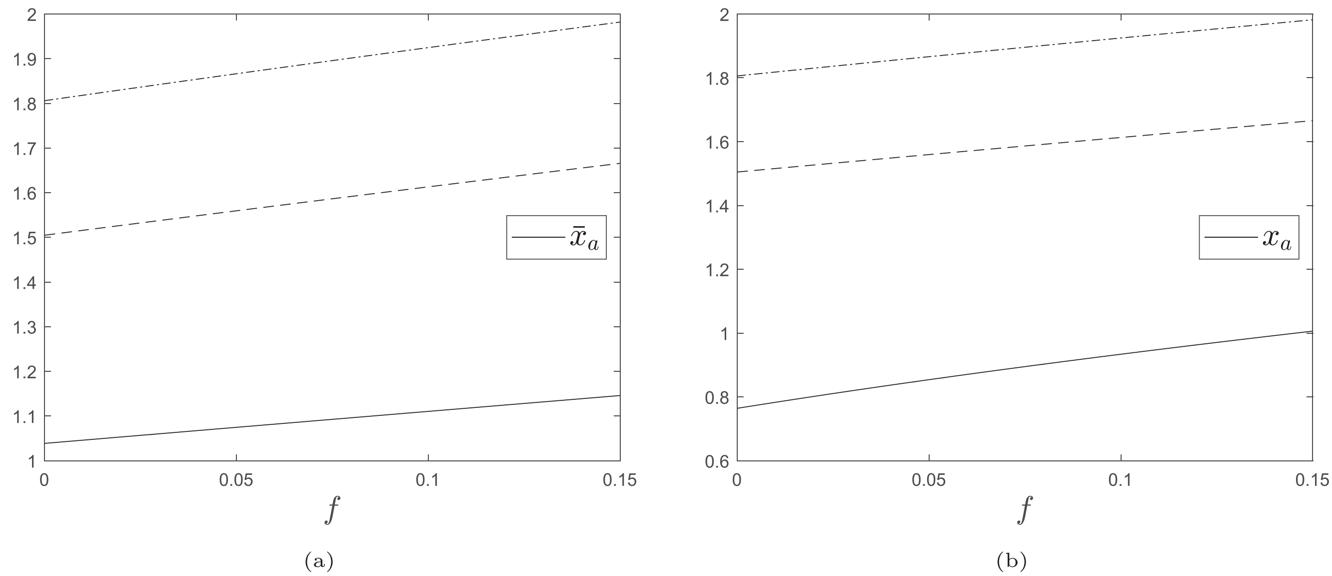

FIGURE 2 | The figure displays the abandonment boundaries of the rigid project (a) and the flexible project (b) as functions of the fixed cost f. Low (dash-dotted lines), intermediate (dashed lines), and high (solid lines) volatility scenarios correspond to the parameter pairs $(\kappa, \sigma) = (0.30, 0.15)$, $(\kappa, \sigma) = (0.15, 0.20)$, and $(\kappa, \sigma) = (0.07, 0.30)$, respectively.

models under examination. Nevertheless, the quantitative sensitivity of each model to changes in the parameters s_{10} and f may differ. To assess this, we compute the variation in each boundary in response to three equidistant changes in the levels of s_{10} and f.

The results, reported in Tables 8 and 9, indicate that the option exercise boundaries are, on average, more sensitive to changes in s_{10} and f under the IGBM and CIR models. This suggests that the operating strategy of the project is comparatively more influenced by changes in the degree of flexibility under these dynamics. However, this effect is less pronounced in the presence of moderate market volatility.

3.6 | Effect on Project Value

We conclude our analysis by examining how the value of the project changes under alternative price models relative to the IGBM benchmark. Table 10 shows that, in terms of direction, the CIR model systematically underestimates the project value, whereas other processes tend to overestimate it. Most

TABLE 8 | The table shows the variations in the optimal option boundaries attributable to changes in the cost of suspending and restarting production, which are assumed to be equal ($s_{10} = s_{01}$).

Panel A: IGBM parameter values $\kappa = 0.15$, $\sigma = 0.20$												
s_{10}	**0.03740**	**0.11210**	**0.15000**	**0.03740**	**0.11210**	**0.15000**	**0.03740**	**0.11210**	**0.15000**			
	$\Delta s(i-1,i)$									$\Delta s(0, i_{\max})$		
Model	x_a			x_s			x_r			x_a	x_s	x_r
IGBM	0	0	0	−10.45359	−4.95496	−1.72654	11.72340	5.20302	1.70482	0	−16.36002	19.54017
CIR	0.04166	0	0	−10.96119	−5.51460	−1.95112	11.44855	4.83792	1.51342	0.04166	−17.51277	18.60862
GBM	0.57559	0.61930	0.25439	−7.06662	−3.17239	−1.10722	7.78099	3.49631	1.15311	1.45590	−11.01116	12.83564
CEV($\beta = -0.5$)	0	0	0	−28.10698	−0.53254	−0.29214	14.88972	0.58658	0.37358	0	−28.69875	15.99536
CEV($\beta = 0$)	0.57559	0.61930	0.25439	−7.06662	−3.17239	−1.10722	7.78099	3.49631	1.15311	1.45590	−11.01116	12.83564
CEV($\beta = 0.5$)	16.69973	0	0	−5.49695	−2.35370	−0.77735	6.97530	1.92260	0.96066	16.69973	−8.43860	10.07943
Panel B: IGBM parameter values $\kappa = 0.07$, $\sigma = 0.30$												
s_{10}	**0.03740**	**0.11210**	**0.15000**	**0.03740**	**0.11210**	**0.15000**	**0.03740**	**0.11210**	**0.15000**			
	$\Delta s(i-1,i)$									$\Delta s(0, i_{\max})$		
Model	x_a			x_s			x_r			x_a	x_s	x_r
IGBM	1.35442	0.94585	2.81756	−13.19776	−5.95605	−2.05406	15.88390	6.95249	2.30076	5.19581	−20.04452	26.79229
CIR	3.11661	3.26459	1.32152	−13.36693	−6.46039	−2.27964	14.67535	6.14198	2.02417	7.89015	−20.81109	24.18249
GBM	0.50658	0.64432	0.26271	−9.17591	−4.13131	−1.38364	10.44989	4.64786	1.53479	1.41991	−14.13289	17.35741
CEV($\beta = -0.5$)	4.28980	0.56603	0.35265	−3.36204	−18.05428	−1.28403	0.24282	−0.55176	1.36144	0	−21.82616	1.04693
CEV($\beta = 0$)	0.73766	0.77788	0.32002	−8.42714	−3.57785	−1.25121	10.93483	3.21423	1.47974	1.84616	−12.80825	16.19484
CEV($\beta = 0.5$)	5.89409	0.45740	0.19328	−5.49695	−2.35370	−0.77735	10.75582	5.03267	1.67462	6.58406	−13.48549	18.27787

Note: For each boundary, marginal variations are denoted by $\Delta s(i-1, i)$, with the starting point at $s_{10} = 0$. Cumulative variations $\Delta s(0{,}0.15)$ are reported in the last three columns. All values are expressed in percentage terms.

TABLE 9 | The table shows the variations in the optimal option boundaries attributable to changes in the fixed cost of the project, f.

Panel A: IGBM parameter values $\kappa = 0.15$, $\sigma = 0.20$								
f	**0.03740**	**0.11210**	**0.15000**	**0.03740**	**0.11210**	**0.15000**		
				$\Delta f(i-1, i)$			$\Delta f(0, i_{\max})$	
Model		$\bar{x}_a$			x_a		$\bar{x}_a$	x_a
IGBM	2.72516	5.18051	2.45069	2.72516	5.18051	2.45069	10.69474	10.69474
CIR	3.15427	6.19868	2.84836	3.15427	6.19868	2.84836	12.66881	12.66881
GBM	1.78993	3.48016	1.72154	2.91156	5.20563	2.31237	7.14571	10.77233
CEV($\beta = -0.5$)	13.67659	8.01367	2.45705	16.74570	−33.42168	61.85193	8.46294	8.46294
CEV($\beta = 0$)	1.78993	3.48016	1.72154	2.91156	5.20563	2.31237	7.14571	10.77233
CEV($\beta = 0.5$)	1.54700	3.03750	1.48661	1.54700	3.03750	1.48661	6.18696	6.18696
Panel B: IGBM parameter values $\kappa = 0.07$, $\sigma = 0.30$								
f	**0.03740**	**0.11210**	**0.15000**	**0.03740**	**0.11210**	**0.15000**		
				$\Delta f(i-1, i)$			$\Delta f(0, i_{\max})$	
Model		$\bar{x}_a$			x_a			
IGBM	2.58969	5.00339	2.40093	9.09482	14.55516	5.76519	10.30899	32.17872
CIR	3.47684	6.95151	3.22888	9.64529	15.62389	5.85537	14.24345	34.19936
GBM	1.78167	3.49472	1.71348	4.02777	7.22604	3.21931	7.14361	15.13583
CEV($\beta = -0.5$)	32.08100	5.90730	2.77681	16.74570	−33.42168	61.85193	9.31622	18.49531
CEV($\beta = 0$)	1.78098	3.49476	1.71347	3.21738	5.73899	2.57007	7.14292	11.94602
CEV($\beta = 0.5$)	1.37001	2.65260	1.29626	2.87468	5.20078	2.34471	5.40783	10.76252

Note: For each boundary, marginal variations are denoted by $\Delta f(i-1, i)$, with the starting point at $f = 0$. Cumulative variations $\Delta f(0{,}0.15)$ are reported in the last three columns. All values are expressed in percentage terms.

TABLE 10 | This table shows the variation in the value of an active project when computed under alternative price processes, as compared to the IGBM benchmark.

Scenario	**$\kappa = 0.30$, $\sigma = 0.15$**		**$\kappa = 0.15$, $\sigma = 0.20$**		**$\kappa = 0.07$, $\sigma = 0.30$**	
Model	$\boldsymbol{\Delta V_1^r(x)}$	$\boldsymbol{\Delta V_1^f(x)}$	$\boldsymbol{\Delta V_1^r(x)}$	$\boldsymbol{\Delta V_1^f(x)}$	$\boldsymbol{\Delta V_1^r(x)}$	$\boldsymbol{\Delta V_1^f(x)}$
IGBM	10.01708	10.01708	10.58344	10.58344	13.80811	13.99732
CIR	−0.12128	−0.12128	−2.07846	−2.07846	−15.61073	−17.23415
GBM	33.93756	33.93756	37.30910	36.82929	31.38040	31.16004
CEV($\beta = -0.5$)	23.84919	23.84919	23.93548	23.93547	15.45188	13.73292
CEV($\beta = 0$)	−0.17028	−0.17028	37.30910	36.82929	2.14315	0.45043
CEV($\beta = 0.5$)	6.19184	6.19184	21.09373	21.09373	50.18965	51.46859

Note: The current price level is $x_0 = 2.00$ across all models and scenarios. The value of the active project under IGBM is reported in the first row and is expressed in monetary terms, while the variations are expressed in percentage terms.

importantly, the magnitude of the error appears to increase monotonically with market volatility when the CIR or CEV model with positive β is considered. The latter, in particular, yields a comparatively unreliable estimate of project value in the high-variance scenario. For the CEV and GBM models, the largest discrepancies arise in the intermediate-volatility case. Notably, the CEV($\beta = 0$) model offers the most robust estimates across extreme variance scenarios, accommodating both low and high volatility effectively.

It is interesting to observe that these results are nearly opposite to those obtained for the project's strategic behaviour. This highlights the importance of clearly identifying the modelling objective—whether the focus is on valuation or on determining the optimal strategy—when developing a real options framework. We do not observe any substantial differences between the responses from the rigid and flexible projects.

4 | Conclusions

An increasing body of literature has questioned the reliance on geometric Brownian motion in real options models, highlighting the importance of mean reversion and its substantial influence on investment probabilities.

In this work, we analyse four price processes and introduce a comparative framework for evaluating production projects with multiple embedded options, namely, suspension, resumption, and abandonment. We show that the price process specification significantly affects the project dynamics, although simpler models can remain effective under certain conditions with minimal strategic impact. A key contribution of our study, compared to the existing literature, lies in the use of a benchmark model. By calibrating the parameters of all alternative price processes to this benchmark, we ensure a meaningful comparison. We investigate the strategic implications for the operating policies of both flexible and rigid projects, focusing on three core aspects relevant to long-term projects: determining optimal switching price levels (*ex-ante* analysis), evaluating the probability of exercising real options in the short term, and analysing the timing of managerial decisions (*ex-post* analysis).

Our results show that in intermediate environments, where the effects of mean reversion and variance tend to offset each other, the use of models other than the benchmark has only a limited impact on project strategy. While this may lead to a suboptimal ex ante strategy, the ex post consequences remain minor, with only modest deviations in short- and long-term managerial actions. This suggests that simpler models, if properly calibrated, can be adopted without substantial loss of accuracy. However, in extreme settings characterised by either high volatility or strong mean reversion, this conclusion no longer holds. In particular, approximating strongly mean-reverting processes with models that omit this feature is inadvisable. This is mostly evident in commodity—especially energy—markets, which consistently exhibit pronounced volatility, mean-reverting behaviour, and stylized features such as seasonality and price spikes.

A central takeaway is the striking variation between models' performance in project valuation and their implications for strategic behaviour. For instance, while the CIR model systematically underestimates project value as market volatility increases, the CEV($\beta = 0$) model delivers more robust estimates across volatility scenarios. Interestingly, these valuation patterns are markedly different from those observed in optimal exercise strategies across models. This discrepancy underscores the need to define the modelling objective clearly—whether the priority is accurate valuation or optimal strategic decision-making—when constructing real options frameworks. Notably, these insights apply consistently to both rigid and flexible project settings.

In an environment increasingly shaped by geopolitical, climatic, and health-related shocks, managerial flexibility, effectively captured through real options, becomes particularly valuable. Future research could extend our framework by applying it to specific international contexts. Moreover, while our analysis assumes a perpetual project duration, short-term decisions may be better addressed through reinforcement learning, which provides computable and interpretable estimates of both option values and optimal exercise strategies.

Acknowledgements

The authors would like to thank the three anonymous reviewers and the Editor-in-Chief, whose valuable comments contributed significantly to the final form of this research paper. Data are available from the authors upon request. The authors declare no competing interests. Finally, the majority of the first author's research was conducted during her PhD studies at Bayes Business School.

Conflicts of Interest

The authors declare no conflicts of interest.

Data Availability Statement

The data that support the findings of this study are available from the corresponding author upon reasonable request.

Endnotes

[1] For decision-makers to make optimal choices, both the utility and the marginal utility of remaining in the continuation region, evaluated at the optimal stopping point, must equal those of switching to one of the alternatives. These requirements give rise to boundary conditions known as the *value-matching* and *smooth-pasting* conditions. More details can be found in Dixit and Pindyck (1994, 130–132).

References

Abramowitz, M., and I. A. Stegun. 1972. *Handbook of Mathematical Functions With Formulas, Graphs and Mathematical Tables*. Dover Publications.

Amici, G., G. Fusai, A. M. Gambaro, and D. Marazzina. 2025. "Navigating Supply Shocks: Sector Resilience and Production Prices Through Stochastic Input–Output Modeling." Working paper, University of Eastern Piedmont.

Azevedo, A., P. J. Pereira, and A. Rodrigues. 2019. "Foreign Direct Investment With Tax Holidays and Policy Uncertainty." *International Journal of Finance and Economics* 24, no. 2: 727–739.

Bessembinder, H., J. F. Coughenour, P. J. Seguin, and M. M. Smoller. 1995. "Mean Reversion in Equilibrium Asset Prices: Evidence From the Futures Term Structure." *Journal of Finance* 50, no. 1: 361–375.

Bhattacharya, S. 1978. "Project Valuation With Mean-Reverting Cash Flow Streams." *Journal of Finance* 33, no. 5: 1317–1331.

Black, F. 1976. "Studies of Stock Price Volatility Changes." In *Proceedings of the 1976 Meeting of the Business and Economic Statistics Section*, 177–181. American Statistical Association.

Boston Consulting Group. 2023. "Harnessing the Tectonic Global Shift in Manufacturing." Technical Report.

Čermák, M. 2017. "Leverage Effect and Stochastic Volatility in the Agricultural Commodity Market Under the CEV Model." *Acta Universitatis Agriculturae et Silviculturae Mendelianae Brunensis* 65, no. 5: 1671–1678.

Chan, K. C., G. A. Karolyi, F. A. Longstaff, and A. B. Sanders. 1992. "An Empirical Comparison of Alternative Models of the Short-Term Interest Rate." *Journal of Finance* 47, no. 3: 1209–1227.

Chi, T., J. Li, L. G. Trigeorgis, and A. E. Tsekrekos. 2019. "Real Options Theory in International Business." *Journal of International Business Studies* 50, no. 4: 525–553.

Cox, J. C. 1975. "Notes on Option Pricing I: Constant Elasticity of Variance Diffusions." Working Paper, Stanford University, Graduate School of Business.

Cox, J. C., J. E. Ingersoll, and S. A. Ross. 1985. "A Theory of the Term Structure of Interest Rates." *Econometrica* 53: 385–407.

Dangerfield, C., A. Whalley, and G. C. Hanley. 2018. "What a Difference a Stochastic Process Makes: Epidemiological-Based Real Options Models of Optimal Treatment of Disease." *Environmental and Resource Economics* 70, no. 3: 691–711.

Davydov, D., and V. Linetsky. 2001. "Pricing and Hedging Path-Dependent Options Under the CEV Process." *Management Science* 47, no. 7: 949–965.

Deloitte. 2024. "Global Supply Chain Resilience Amid Disruptions." Technical Report.

Dias, J. C., M. Larguinho, and C. A. Braumann. 2015. "Entry and Exit Decisions Under Uncertainty for a Generalized Class of One-Dimensional Diffusions." Proceedings of the 19th International Conference on Real Options: Theory Meets Practice.

Dias, J. C., and J. P. V. Nunes. 2011. "Pricing Real Options Under the Constant Elasticity of Variance Diffusion." *Journal of Futures Markets* 31: 230–250.

Dixit, A. 1989. "Entry and Exit Decisions Under Uncertainty." *Journal of Political Economy* 97, no. 3: 620–638.

Dixit, A., and R. Pindyck. 1994. *Investment Under Uncertainty*. Princeton University Press.

European Investment Bank. 2025. "Shock Waves From Turbulent Times: How EU Businesses Recalibrate Supply Chains." Technical Report, European Investment Bank.

Ewald, C., and W. Wang. 2010. "Irreversible Investment With Cox–Ingersoll–Ross Type Mean Reversion." *Mathematical Social Sciences* 59, no. 3: 314–318.

Fama, E., and K. French. 2000. "Forecasting Profitability and Earnings." *Journal of Business* 73, no. 2: 161–175.

Geman, H. 2008. *Commodities and Commodity Derivatives: Modeling and Pricing for Agriculturals, Metals and Energy*. John Wiley & Sons.

Geman, H., and Y. F. Shih. 2008. "Modeling Commodity Prices Under the CEV Model." *Journal of Alternative Investments* 11, no. 3: 65–84.

Glover, K. J., and G. Hambusch. 2016. "Leveraged Investments and Agency Conflicts When Cash Flows Are Mean Reverting." *Journal of Economic Dynamics and Control* 67, no. C: 1–21.

Guthrie, G. 2009. *Real Options in Theory and Practice*. Oxford University Press.

Gutiérrez, Ó. 2021. "Real Options and the Perverse Effect of Interest Rates on Investment Timing." *International Journal of Finance and Economics* 26, no. 3: 3984–3996.

Ipsmiller, E., K. D. Brouthers, and D. Dikova. 2021. "Which Export Channels Provide Real Options to SMEs?" *Journal of World Business* 56, no. 6: 101,245.

Kulatilaka, N. 1988. "Valuing the Flexibility of Flexible Manufacturing Systems." *IEEE Transactions on Engineering Management* 35, no. 4: 250–257.

Kyriakou, I., R. Brignone, and G. Fusai. 2023. "Unified Moment-Based Modeling of Integrated Stochastic Processes." *Operations Research* 72, no. 4: 1630–1653.

Le Guenedal, T., and P. Tankov. 2025. "Corporate Debt Value Under Transition Scenario Uncertainty." *Mathematical Finance* 35, no. 1: 40–73.

Lebedev, N. N. 1972. *Special Functions & Their Applications*. Dover Publications Translated by Richard A. Silverman.

Li, N., A. Ker, A. G. Sam, and S. Aradhyula. 2017. "Modeling regime-dependent agricultural commodity price volatilities." *Agricultural Economics* 48, no. 6: 683–691.

Lund, D. 1993. "The Lognormal Diffusion Is Hardly an Equilibrium Price Process for Exhaustible Resources." *Journal of Environmental Economics and Management* 25, no. 3: 235–241.

Metcalf, G., and K. Hassett. 1995. "Investment Under Alternative Return Assumptions Comparing Random Walks and Mean Reversion." *Journal of Economic Dynamics and Control* 19, no. 8: 1471–1488.

Prokopczuk, M., A. Stancu, and L. Symeonidis. 2019. "The Economic Drivers of Commodity Market Volatility." *Journal of International Money and Finance* 98: 102,063.

Ritchken, P., and Q. Wu. 2021. "Capacity Investment, Production Flexibility, and Capital Structure." *Production and Operations Management* 30: 4593–4613.

Roncoroni, A., G. Fusai, and M. Cummins. 2015. *Handbook of Multi-Commodity Markets and Products: Structuring, Trading and Risk Management*. Wiley.

Rotondi, F. 2025a. "Linking Futures and Options Pricing in the Natural Gas Market." *Risks* 13: 107.

Rotondi, F. 2025b. "Seasonality and Spikes in the Natural Gas Market." *Energy Economics* 148: 108586.

Sarkar, S. 2003. "The Effect of Mean Reversion on Investment Under Uncertainty." *Journal of Economic Dynamics and Control* 28, no. 2: 377–396.

Sarkar, S., and F. Zapatero. 2003. "The Trade-Off Model With Mean Reverting Earnings: Theory and Empirical Tests." *Economic Journal* 113, no. 490: 834–860.

Schwartz, E. 1997. "The Stochastic Behavior of Commodity Prices: Implications for Valuation and Hedging." *Journal of Finance* 52, no. 3: 923–973.

Tong, T., and J. Reuer. 2007. "Real Options in Multinational Corporations: Organizational Challenges and Risk Implications." *Journal of International Business Studies* 38: 215–230.

Tsekrekos, A. E. 2010. "The Effect of Mean Reversion on Entry and Exit Decisions Under Uncertainty." *Journal of Economic Dynamics and Control* 34, no. 4: 725–742.

Tsekrekos, A. E. 2013. "Irreversible Exit Decisions Under Mean-Reverting Uncertainty." *Journal of Economics* 110, no. 1: 5–23.

Tvedt, J. 2022. "Optimal Entry and Exit Decisions Under Uncertainty and the Impact of Mean Reversion." *Operations Research Forum* 3: 1–21.

Uhlenbeck, G. E., and L. S. Ornstein. 1930. "On the Theory of the Brownian Motion." *Physical Review* 36, no. 5: 823–841.

Zhao, B. 2009. "Inhomogeneous Geometric Brownian Motions." Working Paper, City University London.

Appendix A

Derivations

In what follows, we outline the derivation of the project's value function presented in Section 2.3. Additionally, we demonstrate how to apply the value-matching and smooth-pasting conditions, following Dixit and Pindyck (1994).

General Solution of Homogeneous Equation

We adopt a standard approach that transforms our equations into a form with a known solution, specifically, the confluent differential equation, whose solution is expressed in terms of hypergeometric functions of the first and second kind (see, e.g., Tsekrekos 2010).

Let f, h, V be twice differentiable functions of x. Consider the confluent differential equation

$$V'' + \left[\frac{2A}{x} + 2f' + \frac{\gamma h'}{h} - h' - \frac{h''}{h'}\right]V' + \left[\left(\frac{\gamma h'}{h} - h' - \frac{h''}{h'}\right)\left(\frac{A}{x} + f'\right) + \frac{A(A-1)}{x^2} + \frac{2Af'}{x} + f'' + [f']^2 - \frac{\alpha [h']^2}{h}\right]V = 0, \tag{A.1}$$

whose solution is known to be (see Abramowitz and Stegun 1972, eqs. (13.1.36) and (13.1.37))

$$c_1 e^{-f}\Phi(\alpha, \gamma; h)x^{-A} + c_2 e^{-f}\Psi(\alpha, \gamma; h)x^{-A}, \tag{A.2}$$

where

$$\Phi(\alpha, \gamma; h) = \sum_{k=0}^{\infty} \frac{(\alpha)_k h^k}{(\gamma)_k k!}, \quad |h| < \infty, \alpha \in \mathbb{C}, \gamma \in \mathbb{C} \setminus \mathbb{Z}^-$$

is a confluent hypergeometric function of the first kind, and

$$\Psi(\alpha, \gamma; h) = \frac{\Gamma(1-\gamma)}{\Gamma(1+\alpha-\gamma)}\Phi(\alpha, \gamma; h) + \frac{\Gamma(\gamma-1)}{\Gamma(\alpha)}h^{1-\gamma}\Phi(1+\alpha-\gamma, 2-\gamma; h) \tag{A.3}$$

is a confluent hypergeometric function of the second kind. Replacing (A.3) in (A.2) yields

$$pe^{-f}\Phi(\alpha, \gamma; h)x^{-A} + qe^{-f}\Phi(1+\alpha-\gamma, 2-\gamma; h)x^{1-\gamma-A} \tag{A.4}$$

with $p = c_1 + c_2\Gamma(1-\gamma)/\Gamma(1+\alpha-\gamma)$ and $q = c_2\Gamma(\gamma-1)/\Gamma(\alpha)$.

The homogeneous parts of the ordinary differential equations obtained for IGBM, CIR, and CEV ($\mu \neq 0$) are

$$\frac{\sigma^2}{2}x^2V'' + \kappa(\theta - x)V' - rV = 0 \text{ for IGBM,} \tag{A.5}$$

$$\frac{\sigma^2}{2}xV'' + \kappa(\theta - x)V' - rV = 0 \text{ for CIR,} \tag{A.6}$$

$$\frac{\sigma^2}{2}x^{2\beta+2}V'' + \mu xV' - rV = 0 \text{ for CEV.} \tag{A.7}$$

These can be rewritten in the confluent form

$$xV'' + \left[\frac{2\kappa\theta}{\sigma^2 x} - \frac{2\kappa}{\sigma^2}\right]V' - \frac{2r}{\sigma^2 x}V = 0 \text{ for IGBM,} \tag{A.8}$$

$$xV'' + \left[\frac{2\kappa\theta}{\sigma^2} - \frac{2\kappa x}{\sigma^2}\right]V' - \frac{2r}{\sigma^2}V = 0 \text{ for CIR,} \tag{A.9}$$

$$\frac{x}{|\beta|}V'' + \frac{2\mu\sigma}{\sigma^2 |\beta| x^{2\beta}}V' - \frac{2r}{\sigma^2 |\beta| x^{2\beta+1}}V = 0 \text{ for CEV.} \tag{A.10}$$

Thus, Equations (A.8–A.10) conform to the confluent differential equation with appropriate choices of h:

$$h = \begin{cases} \dfrac{2\kappa\theta}{\sigma^2 x} & \text{for IGBM} \\ \dfrac{2\kappa x}{\sigma^2} & \text{for CIR} \\ \dfrac{\mu}{|\beta|\sigma^2 x^{2\beta}} & \text{for CEV} \end{cases}.$$

Let $f = 0, \xi = -A$, and substitute the relevant expression for h into (A.1) to obtain, first, for IGBM

$$V'' + \left[2 - \gamma - 2\xi + \frac{2\kappa\theta}{\sigma^2 x}\right]V' + \left[\frac{\gamma\xi - 2\xi + \xi(1+\xi)}{x} - \frac{2\kappa\theta(\alpha+\xi)}{\sigma^2 x^2}\right]V = 0, \tag{A.11}$$

second, for CIR

$$V'' + \left[\gamma - 2\xi - \frac{2\kappa x}{\sigma^2}\right]V' + \left[-\frac{2(\alpha-\xi)\kappa}{\sigma^2} - \xi\frac{(\gamma-1-\xi)}{x}\right]V = 0, \tag{A.12}$$

third, for CEV ($\beta > 0, \mu \neq 0$)

$$\frac{x}{\beta}V'' + \left[2(1-\gamma) + \frac{1-2\xi}{\beta} + \frac{\mu}{\beta\sigma^2 x^{2\beta}}\right]V' + \left[\frac{-2\xi(1-\gamma)}{x} + \frac{\xi^2}{\beta x} - \frac{4\mu}{\beta\sigma^2 x^{2\beta+1}}\right]V = 0. \tag{A.13}$$

To match the forms (A.8–A.10) with (A.11–A.13), we equate the coefficients of V'', V' and V. This leads to systems of three equations for each model and the associated solutions. First, for IGBM

$$\begin{cases} 2 - \gamma - 2\xi = -\dfrac{2\kappa}{\sigma^2} & \xi_{1,2} = \dfrac{\sigma^2 + 2\kappa \pm \sqrt{\left(\sigma^2 + 2\kappa\right)^2 + 8r\sigma^2}}{2\sigma^2} \\ \gamma\xi - 2\xi + \xi(1+\xi) = -\dfrac{2r}{\sigma^2} & \Rightarrow \gamma_{1,2} = 2 - 2\xi_{1,2} + \dfrac{2\kappa}{\sigma^2} \\ -\dfrac{2\kappa\theta(\alpha+\xi)}{\sigma^2 x^2} = 0 & \alpha_{1,2} = -\xi_{1,2} \end{cases},$$

second, for CIR

$$\begin{cases} \gamma - 2\xi = \dfrac{2\kappa\theta}{\sigma^2} & \xi_1 = 0, \quad \xi_2 = 1 - \dfrac{2\kappa\theta}{\sigma^2} \\ -\dfrac{2\alpha\kappa}{\sigma^2} + \dfrac{2\xi\kappa}{\sigma^2} = -\dfrac{2r}{\sigma^2} & \Rightarrow \gamma_1 = \dfrac{2\kappa\theta}{\sigma^2}, \quad \gamma_2 = 2 - \dfrac{2\kappa\theta}{\sigma^2} \\ -\gamma\xi + \xi^2 + \xi = 0 & \alpha_1 = \dfrac{r}{\kappa}, \quad \alpha_2 = \dfrac{-2\kappa^2\theta + \sigma^2(\kappa + r)}{\sigma^2\kappa} \end{cases},$$

third, for CEV

$$\begin{cases} -\dfrac{2\xi}{\beta} - 2\gamma + \dfrac{1}{\beta} + 2 = 0 & \xi_1 = 1, \quad \xi_2 = 0 \\ \dfrac{\xi^2}{\beta \mathrm{x}} + \dfrac{2\xi\gamma}{x} - \dfrac{2\xi}{x} = 0 & \Rightarrow \gamma_1 = -\dfrac{1-2\beta}{2\beta}, \quad \gamma_2 = -\dfrac{-2\beta-1}{2\beta} \\ -\dfrac{4\alpha\mu x^{-2\beta-1}}{\sigma^2} - \dfrac{2\xi\mu x^{-2\beta-1}}{\beta\sigma^2} + \dfrac{2rx^{-2\beta-1}}{\beta\sigma^2} = 0 & \alpha_1 = -\dfrac{\mu-r}{2\beta\mu}, \quad \alpha_2 = \dfrac{r}{2\beta\mu} \end{cases}. \tag{A.14}$$

Equations (A.11–A.13) therefore have solutions of the form (A.4) for the corresponding parameter triplet $\{\xi_1, \gamma_1, \alpha_1\}$. The second solution set $\{\xi_2, \gamma_2, \alpha_2\}$ is related through

$$\alpha_2 = 1 + \alpha_1 - \gamma_1,$$
$$\gamma_2 = 2 - \gamma_1,$$
$$\xi_2 = 1 - \gamma_1 - \xi_1.$$

We now focus on the CEV model with $\beta < 0$ and $\mu \neq 0$. The steps mirror those leading to (A.14), but we set $f = h$ in (A.1). The resulting parameters in (A.4) become

$$\xi_1 = 1, \quad \xi_2 = 0; \quad \gamma_1 = -\frac{1-2\beta}{2\beta}, \quad \gamma_2 = -\frac{-2\beta-1}{2\beta};$$
$$\alpha_1 = -\frac{r-2\beta\mu}{2\beta\mu}, \quad \alpha_2 = -\frac{r-2\beta\mu-\mu}{2\beta\mu}.$$

We have so far assumed $\mu \neq 0$. The special case $\mu = 0$ under the CEV model is straightforward. Following Davydov and Linetsky (2001), Equation (A.7) reduces to a modified Bessel equation. Its two linearly independent solutions are $x^{1/2}I_\nu(z)$ and $x^{1/2}K_\nu(z)$, where $I_\nu(z), K_\nu(z)$ are modified Bessel functions with

$$z = \frac{\sqrt{2r}x^{-\beta}}{\sigma\,|\,\beta\,|}, \quad \nu = \frac{1}{2\,|\,\beta\,|}.$$

Using the relationship between modified Bessel and hypergeometric functions (cf. Lebedev 1972, eqs. (9.13.14) and (9.13.15)),

$$I_\nu(z) = \frac{(z/2)^\nu}{\Gamma(\nu+1)}e^{-z}\Phi\left(\nu+\frac{1}{2}, 2\nu+1; 2z\right) \quad |\arg z| < \pi, \quad \text{(A.15)}$$

$$K_\nu(z) = \sqrt{\pi}(2z)^\nu e^{-z}\Psi\left(\nu+\frac{1}{2}, 2\nu+1; 2z\right) \quad |\arg z| < \pi. \quad \text{(A.16)}$$

Combining these with (A.3), the general solution to (A.7) when $\mu = 0$ can still be written in the form of (A.4):

$$V(x) = \left[p\Phi(\alpha_1, \gamma_1; 2z)x^{\xi_1} + q\Phi(\alpha_2, \gamma_2; 2z)x^{\xi_2}\right]^z e^{-z},$$

where

$$\xi_1 = 1, \quad \xi_2 = 0; \quad \gamma_1 = 2\nu + 1, \quad \gamma_2 = 2 - 2\nu; \quad \alpha_1 = \frac{1}{2} + \nu, \quad \alpha_2 = \frac{1}{2} - \nu.$$

Finally, the solution for the GBM model can be derived as a limit case of the IGBM. Consider

$$\mathrm{d}x = \kappa(\theta - x)\mathrm{d}t + \sigma x\mathrm{d}W \quad \text{as} \quad \theta \to 0 \Rightarrow \mathrm{d}x = -\kappa x\mathrm{d}t + \sigma x\mathrm{d}W$$

which is a GBM with drift $-\kappa$. The corresponding ordinary differential equation

$$\frac{\sigma^2}{2}x^2V'' + \mu xV' - rV = 0$$

is thus a special case of (A.5) with $\theta \to 0$ and $\mu = -\kappa$. Consequently, its solution is of the form (A.4). Noting that

$$\theta 0 \underrightarrow{\lim} \frac{2\kappa\theta}{\sigma^2 x} = 0, \quad \chi 0 \underrightarrow{\lim} \Phi(\alpha, \gamma; \chi) = 1$$

the GBM solution simplifies to

$$V(x) = px^{\xi_1} + qx^{\xi_2}$$

with

$$\xi_{1,2} = \frac{\sigma^2 - 2\mu \pm \sqrt{\left(\sigma^2 - 2\mu\right)^2 + 8r\sigma^2}}{2\sigma^2}.$$

Particular Solution

When the project is in the suspended state, the instantaneous cash flow is $-f$, and thus the particular solution is

$$\psi(x) = -\frac{f}{r}$$

regardless of the underlying model.

We now determine $\psi(x)$ for the active state. Since the cash flow function $F(x)$ in (4) is linear in x, we consider a particular solution of the form $y(x) = Ax + B$. Then, $y'(x) = A$, $y''(x) = 0$. This implies that the second derivative term vanishes and only the drift term affects the form of $y(x)$. Hence, the key discriminating factor is whether the underlying process is mean-reverting.

For mean-reverting processes,

$$\kappa(\theta - x)A - r(Ax + B) = -(x - c) \Rightarrow -A(\kappa + r)x + \kappa\theta A - rB = -x + c$$

Solving for A and B yields

$$A = \frac{1}{r+\kappa}, \quad B = \frac{\kappa\theta}{(r+\kappa)r} - \frac{c}{r},$$

thus the particular solution becomes

$$\psi^{MR}(x) = \frac{x}{r+\kappa} + \frac{\kappa\theta}{(r+\kappa)r} - \frac{c}{r}.$$

This expression is equivalent to Equation (15) in Bhattacharya (1978), assuming an infinite time horizon.

For non-mean-reverting processes,

$$\mu xA - r(Ax + B) = -(x - c) \Rightarrow A(\mu - r)x - rB = -x + c.$$

Solving yields

$$A = \frac{1}{r-\mu}, \quad B = -\frac{c}{r},$$

and the particular solution is

$$\psi^{\overline{MR}}(x) = \frac{x}{r-\mu} - \frac{c}{r}.$$

Value-Matching Conditions: Flexible Firm

We begin with the suspension and resumption boundaries, imposing

$$\begin{cases} V_1(x_s) = V_0(x_s) - s_{10} \\ V_0(x_r) = V_1(x_r) - s_{01} \end{cases},$$

which lead to

$$\begin{cases} p_1\Phi\left(\alpha_1;\gamma_1, \dfrac{2\kappa\theta}{\sigma^2 x_s}\right)x_s^{\xi_1} + (p_2 - q_2)\Phi\left(\alpha_2;\gamma_2, \dfrac{2\kappa\theta}{\sigma^2 x_s}\right)x_s^{\xi_2} = \dfrac{f}{r} + \psi^{MR}(x_s) + s_{10} \\ p_1\Phi\left(\alpha_1;\gamma_1, \dfrac{2\kappa\theta}{\sigma^2 x_r}\right)x_r^{\xi_1} + (p_2 - q_2)\Phi\left(\alpha_2;\gamma_2, \dfrac{2\kappa\theta}{\sigma^2 x_r}\right)x_r^{\xi_2} = \dfrac{f}{r} + \psi^{MR}(x_r) - s_{01} \end{cases}.$$

This is a linear system in p_1 and $(p_2 - q_2)$, which we write as $\mathbf{Ax} = \mathbf{b}$:

$$\mathbf{A}=\begin{bmatrix}\Phi\left(\alpha_1,\gamma_1;\dfrac{2\kappa\theta}{\sigma^2x_s}\right)x_s^{\xi_1} & \Phi\left(\alpha_2,\gamma_2;\dfrac{2\kappa\theta}{\sigma^2x_s}\right)x_s^{\xi_2}\\ \Phi\left(\alpha_1,\gamma_1;\dfrac{2\kappa\theta}{\sigma^2x_r}\right)x_r^{\xi_1} & \Phi\left(\alpha_2,\gamma_2;\dfrac{2\kappa\theta}{\sigma^2x_r}\right)x_r^{\xi_2}\end{bmatrix},$$

$$\mathbf{x}=\begin{bmatrix}p_1\\ p_2-q_2\end{bmatrix},\quad \mathbf{b}=\begin{bmatrix}\dfrac{f}{r}+\psi^{MR}(x_s)+s_{10}\\ \dfrac{f}{r}+\psi^{MR}(x_r)-s_{01}\end{bmatrix}.$$

Provided that $\mathbf{A}$ is non-singular, the unique solution is $\mathbf{x}=\mathbf{A}^{-1}\mathbf{b}$.

With p_1 and (p_2-q_2) known, we use the abandonment condition

$$V_0(x_a)=\eta I$$

to solve for q_2 and p_2:

$$p_1\Phi\left(\alpha_1,\gamma_1;\frac{2\kappa\theta}{\sigma^2x_a}\right)x_a^{\xi_1}+p_2\Phi\left(\alpha_2,\gamma_2;\frac{2\kappa\theta}{\sigma^2x_a}\right)x_a^{\xi_2}-\frac{f}{r}=\eta I,$$

from which

$$q_2=\frac{\eta I+\frac{f}{r}-p_1\Phi\left(\alpha_1,\gamma_1;\frac{2\kappa\theta}{\sigma^2x_a}\right)x_a^{\xi_1}-(p_2-q_2)\Phi\left(\alpha_2,\gamma_2;\frac{2\kappa\theta}{\sigma^2x_a}\right)x_a^{\xi_2}}{\Phi\left(\alpha_2,\gamma_2;\frac{2\kappa\theta}{\sigma^2x_a}\right)x_a^{\xi_2}},$$

$$p_2=(p_2-q_2)+q_2.$$

To extend this approach to any of the diffusion models considered, one simply modifies the entries of $\mathbf{A}$, $\mathbf{x}$, and $\mathbf{b}$ accordingly.

Smooth-Pasting Conditions: Flexible Firm

Smooth-pasting conditions are first used to jointly determine the suspension and resumption boundaries x_s and x_r, and then to find the abandonment barrier x_a iteratively.

The smooth-pasting conditions are

$$\begin{cases}V_1'(x_s)=V_0'(x_s)\\ V_0'(x_r)=V_1'(x_r)\end{cases},$$

which become

$$\begin{cases}p_1\phi_1(x_s)+(p_2-q_2)\phi_2(x_s)=\psi^{MR}(x_s)\\ p_1\phi_1(x_r)+(p_2-q_2)\phi_2(x_r)=\psi^{MR}(x_r)\end{cases}. \tag{A.17}$$

Here, $\phi_j(x)$ is the derivative of $\Phi\left(\alpha_j,\gamma_j;\frac{2\kappa\theta}{\sigma^2x}\right)x^{\xi_j}$, and it is given as

$$\phi_j(x)=\left[\xi_j\Phi\left(\alpha_j,\gamma_j;\frac{2\kappa\theta}{\sigma^2x}\right)-\frac{2\alpha_j\kappa\theta}{\gamma_j\sigma^2x}\Phi\left(\alpha_j+1,\gamma_j+1;\frac{2\kappa\theta}{\sigma^2x}\right)\right]x^{\xi_j-1}.$$

This follows from the chain rule applied to the confluent hypergeometric function (cf. Lebedev 1972):

$$\frac{\mathrm{d}}{\mathrm{d}x}\Phi\left(\alpha,\gamma;\frac{2\kappa\theta}{\sigma^2x}\right)=-\frac{\alpha}{\gamma}\Phi\left(\alpha+1,\gamma+1;\frac{2\kappa\theta}{\sigma^2x}\right)\frac{2\kappa\theta}{\sigma^2x^2}.$$

Solving the system in (A.17) gives the optimal boundaries x_s and x_r. Then, using these values, the abandonment threshold x_a is determined from

$$V_0'(x_a)=0\quad\Rightarrow\quad p_1\phi_1(x_a)+p_2\phi_2(x_a)=0.$$